Applied Physics Express **6** (2013) 021101
http://dx.doi.org/**10.7567/APEX.6.021101**

Thermal Conductivity of Amorphous Indium–Gallium–Zinc Oxide Thin Films

Toru Yoshikawa[1], Takashi Yagi[2], Nobuto Oka[1], Junjun Jia[1], Yuichiro Yamashita[2], Koichiro Hattori[2], Yutaka Seino[2], Naoyuki Taketoshi[2], Tetsuya Baba[2], and Yuzo Shigesato[1]*

[1]*Graduate School of Science and Engineering, Aoyama Gakuin University, Sagamihara 252-5258, Japan*
[2]*National Metrology Institute of Japan (NMIJ), National Institute of Advanced Industrial Science and Technology (AIST), Tsukuba, Ibaraki 305-8563, Japan*
E-mail: yuzo@chem.aoyama.ac.jp

Received December 17, 2012; accepted December 29, 2012; published online January 25, 2013

We investigated the thermal conductivity of 200-nm-thick amorphous indium–gallium–zinc-oxide (a-IGZO) films. Films with a chemical composition of In : Ga : Zn = 1 : 1 : 0.6 were prepared by dc magnetron sputtering using an IGZO ceramic target and an Ar–O_2 sputtering gas. The carrier density of the films was systematically controlled from 10^{14} to $>10^{19}$ cm^{-3} by varying the O_2 flow ratio. Their Hall mobility was slightly higher than 10 $cm^2 \cdot V^{-1} \cdot s^{-1}$. Those films were sandwiched between 100-nm-thick Mo layers; their thermal diffusivity, measured by a pulsed light heating thermoreflectance technique, was $\sim 5.4 \times 10^{-7}$ $m^2 \cdot s^{-1}$ and was almost independent of the carrier density. The average thermal conductivity was 1.4 $W \cdot m^{-1} \cdot K^{-1}$.

Amorphous indium–gallium–zinc oxide (a-IGZO) has attracted much attention as a high-performance channel material for thin-film transistors (TFTs) because of its large Hall mobility of up to 10 $cm^2 \cdot V^{-1} \cdot s^{-1}$.[1–7] It is expected that a-IGZO films will be used as the semiconductor layer in TFTs for applications such as OLEDs[8] and flexible electronic paper.[9] Because an appropriate thermal design of such devices is essential for preventing them from overheating or forming short circuits, the thermophysical properties of a-IGZO films is necessary for an effective thermal design.

We already reported the thermal conductivities of amorphous transparent conductive oxide (TCO) films such as amorphous indium–zinc-oxide (a-IZO) films.[10] The thermal conductivity of degenerate a-IZO films is linearly proportional to the electrical conductivity. Carrier transport in a-IGZO is governed by percolation conduction via the overlapping outer *s* orbitals (i.e., conduction band) of In^{4+} and randomly distributed Ga^{3+} and Zn^{2+} ions.[6] When the carrier concentration exceeds 3×10^{18} cm^{-3}, IGZO is in the degenerate state. The behavior of the thermophysical properties of amorphous TCOs near the degenerate state is not well known because carriers associated with oxygen vacancies in IZO films are easily produced and, in turn, the nearly degenerate state becomes unstable. On the other hand, a-IGZO contains Ga–O bonds, which are stronger than Zn–O and In–O bonds, improving the controllability of carrier densities in the nearly degenerate state.

In this study, we measured the thermal diffusivity of a-IGZO films by a pulsed light heating thermoreflectance technique[11–13] to investigate the thermal conductivity of a-IGZO films in the nearly degenerate state. A-IGZO films with a thickness of 200 nm were deposited on unheated synthesized quartz glass substrates by dc magnetron sputtering using an In_2O_3–Ga_2O_3–ZnO ceramic target (Toshima Mfg.) with a molar ratio of In : Ga : Zn = 1 : 1 : 1. The sputtering gas was a mixture of Ar and O_2 gases, where the O_2 flow ratio was varied from 0 to 2%, and the total gas pressure was 0.5 Pa. All of the deposited films showed an amorphous structure as examined by X-ray diffraction analysis (XRD) using Cu $K\alpha_1$ radiation at 40 kV and 20 mA (Shimadzu XRD-6000). The optical transmittance of all the films was greater than 80% in the visible region. Their chemical compositions were determined by electron probe microanalysis (EPMA; JEOL JXA-8200). The result of the EPMA shows evidence of re-evaporation of zinc from the films during the deposition process. The molar ratio of In : Ga : Zn for all the films was roughly 1 : 1 : 0.6, which slightly shifted from that of the ceramic target.

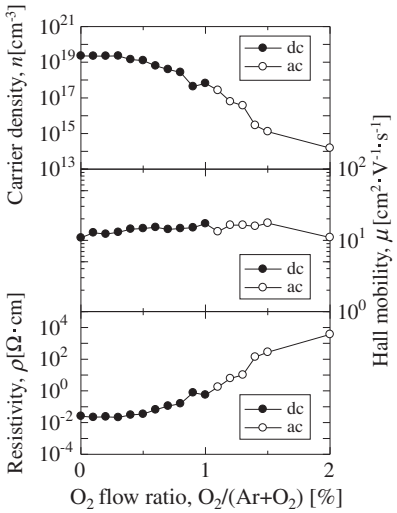

Fig. 1. Carrier density (n), Hall mobility (μ) and resistivity (ρ) of a-IGZO films as functions of O_2 flow ratio during deposition. The applied magnetic field for the Hall measurement was changed from the dc method to the ac method when the resistivity exceeded 1 Ω·cm.

Figure 1 shows the electrical properties of the a-IGZO films as functions of the O_2 flow ratio by a four-point probe method and van der Pauw geometry (Accent HL-5500PC and Toyo ResiTest8300). When the resistivity of the films exceeded 1 Ω·cm, the applied magnetic field for the Hall measurement was changed from the dc method to the ac method, as shown in Fig. 1. The carrier density decreased from 2×10^{19} to 2×10^{14} cm^{-3} with increasing O_2 flow ratio. The resistivity of the films increased from 3×10^{-2} to 4×10^3 Ω·cm with increasing O_2 flow ratio. Since carrier generation in a-IGZO is associated with oxygen vacancies, the increase of the O_2 flow ratio leads to the reduction of the number of oxygen vacancies in the film. The Hall mobility is, however, always higher than 10 $cm^2 \cdot V^{-1} \cdot s^{-1}$.

To measure the thermal diffusivity of the a-IGZO films, we deposited Mo/a-IGZO/Mo layered samples on synthesized quartz glass substrates, where the deposition condi-

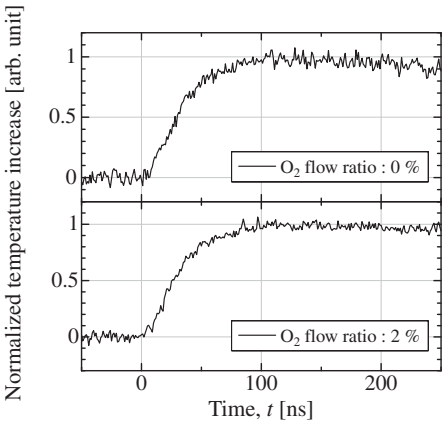

Fig. 2. Normalized transient temperatures of Mo/a-IGZO/Mo three-layered films, where the a-IGZO was deposited at the O_2 flow ratios of 0 and 2%, obtained by the pulsed light heating thermoreflectance technique.

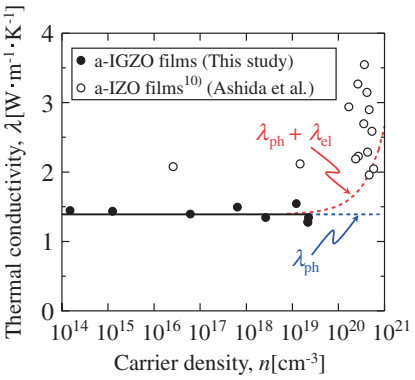

Fig. 3. Thermal conductivities of a-IGZO and a-IZO[10] films as a function of carrier density. A red dashed curve represents estimated thermal conductivity of a-IGZO film derived from sum of the contributions of phonons (λ_{ph}) and electrons (λ_{el}). λ_{el} is calculated using Wiedemann–Franz law, where Lorenz number and Hall mobility are $2.45 \times 10^{-8}\,W{\cdot}\Omega{\cdot}K^{-2}$ and $10.9\,cm^2{\cdot}V^{-1}{\cdot}s^{-1}$, respectively. A blue dashed line shows λ_{ph} of the IGZO films.

tions of the a-IGZO layer such as the mixture gas, thickness and total gas pressure were those mentioned above. The top and bottom Mo layers were each 100 nm thick. We irradiated the samples with a pump laser beam having a wavelength of 1064 nm, a pulse duration of 0.5 ns, a spot size of 300 μm, and a pulse energy of 0.1 μJ at the bottom Mo layer (i.e., Mo/substrate interface) to yield one-dimensional heat flow across the layered sample. Then, the temperature at the surface of the top Mo layer was detected using a probe laser beam with a wavelength of 782 nm, a pulse duration of 0.5 ns, a spot size of 100 μm, and a pulse energy of 2 nJ. The reflected probe beam was detected by a silicon photodiode. The details of the measurement techniques can be found in previous reports.[11,14)]

Figure 2 shows typical transient temperatures of the Mo/a-IGZO/Mo films, where the a-IGZO layers were deposited at the O_2 flow ratios of 0 and 2%. There is no significant difference between the two transient temperature curves. As seen in Fig. 1, those two films have very different electrical properties. For example, the carrier density and resistivity of the films deposited at an O_2 flow ratio of 0% are $>10^{19}\,cm^{-3}$ and $3 \times 10^{-2}\,\Omega{\cdot}cm$, while those of the film deposited at an O_2 flow ratio of 2% are $10^{14}\,cm^{-3}$ and $>10^3\,\Omega{\cdot}cm$, respectively. The speed of the temperature increase corresponds to the thermophysical properties of the constituent layers. Therefore, it can be considered that the electrical properties of the films do not significantly influence the thermophysical properties. The thermal diffusivities of the a-IGZO films were analyzed by the areal heat diffusion time method.[11)] The thermal boundary resistance (TBR) between the a-IGZO and Mo layers can be negligible in this study because the TBR value is considered to be sufficiently small in comparison with the total thermal resistance.[13,15)] The thermal diffusivity of the a-IGZO films was $5.4 \times 10^{-7}\,m^2{\cdot}s^{-1}$, which was almost constant against the O_2 flow ratio, i.e., independent of the carrier density and the resistivity.

The thermal conductivity of the a-IGZO films was calculated from their measured thermal diffusivity and density as well as their estimated specific heat capacity. The density of the a-IGZO film was determined to be $6.0\,g{\cdot}cm^{-3}$ by X-ray reflection analysis.[16)] The specific heat capacity was $426\,J{\cdot}kg^{-1}{\cdot}K^{-1}$, which was deduced from the weighted average of the specific heat capacities[17,18)] of In_2O_3, Ga_2O_3, and ZnO according to the chemical composition of the films analyzed by EPMA. Figure 3 shows the thermal conductivity (λ) of the a-IGZO films as a function of the carrier density. The data for a-IZO films reported by Ashida et al. are also plotted in this figure.[10)] As the carrier density becomes smaller than $10^{18}\,cm^{-3}$, TCO films become from a nearly degenerate state to a non-degenerate state. In this region, the thermal conductivities of the a-IGZO films show a constant value of $1.4\,W{\cdot}m^{-1}{\cdot}K^{-1}$. For the a-IZO films, the thermal conductivities spread from 2 to $3.5\,W{\cdot}m^{-1}{\cdot}K^{-1}$, when the carrier density is larger than $10^{20}\,cm^{-3}$. Those a-IZO films are in the degenerate state and free electrons carry heat conduction. However, below the carrier density of $10^{19}\,cm^{-3}$, the a-IZO films also show a constant thermal conductivity. Thus, the carrier density of around 10^{19}–$10^{20}\,cm^{-3}$ is considered to be a threshold of heat conduction by free electrons. A red dashed curve in Fig. 3 represents an estimated thermal conductivity derived from sum of the contributions of phonons (λ_{ph}) and electrons (λ_{el}). λ_{el} is calculated using Wiedemann–Franz law, where Lorenz number and Hall mobility are $2.45 \times 10^{-8}\,W{\cdot}\Omega{\cdot}K^{-2}$ and $10.9\,cm^2{\cdot}V^{-1}{\cdot}s^{-1}$, respectively. Furthermore, in the non-degenerate state ($<3 \times 10^{18}\,cm^{-3}$ in carrier density), the thermal conductivity of the a-IGZO films is clearly smaller than that of the a-IZO films. This fact implies that both amorphous TCO films have different λ_{ph} magnitudes.

Table I shows the λ_{ph} values of In_2O_3-based TCO films. Ashida et al. reported the λ_{ph} values of crystal ITO (c-ITO)[19)] and a-IZO films.[10)] The λ_{ph} of an amorphous ITO (a-ITO) film is obtained from Ref. 13. The λ_{ph} values of amorphous films are less than half of that of the c-ITO film, which is caused by an increase in phonon scattering due to their anharmonic structure. Among the amorphous TCO films, the a-IGZO film exhibits the smallest λ_{ph}. There can be two reasons for the a-IGZO films to show a minimum value of λ_{ph}. One is that the number of constituent cations in the a-IGZO films, such as In, Ga, and Zn ions, is larger than that in the a-ITO and a-IZO films. For example, Andrews et al.[20)] reported that nanowires of crystal IGZO exhibit the thermal conductivity of $3.3\,W{\cdot}m^{-1}{\cdot}K^{-1}$, which is slightly

Table I. Thermal conductivities carried by phonons (λ_{ph}) for In_2O_3-based TCO films. Chemical compositions except for the a-IGZO film were those of the sputtering target estimated from Refs. 10, 13, and 19.

TCOs	c-ITO[19]	a-ITO[13]	a-IZO[10]	a-IGZO
λ_{ph} ($W \cdot m^{-1} \cdot K^{-1}$)	3.95	2.2–1.8	1.85	1.4
Chemical composition	In : Sn = 1 : 0.1	In : Sn = 1 : 0.1	In : Zn = 1 : 0.2	In : Ga : Zn = 1 : 1 : 0.6

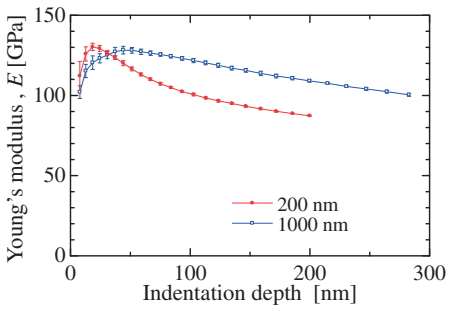

Fig. 4. Young's moduli of a-IGZO films with thicknesses of 200 and 1000 nm as a function of indentation depth.

lower than that of crystal IZO, 3.5 $W \cdot m^{-1} \cdot K^{-1}$ measured by Kaga et al.[21] The other is that our a-IGZO films heavily contain Ga and Zn ions. Eguchi et al.[22] explained that Zn ions in a-IZO films improve the stability of amorphous structure because existence of Zn ions prevents In ions from being ordered as in a bixbyite In_2O_3 crystal.

To classify the amorphous TCO films in terms of phonon heat conduction, we estimated the mean free path of phonons (l_{ph}) for the a-IGZO films by the following equation:

$$\lambda_{ph} = \frac{1}{3} C v l_{ph}, \quad (1)$$

where C is heat capacity per unit volume and v is the average phonon velocity. In this study, we assume that v is the sound velocity calculated from Young's modulus E and the density ρ_d by the following equation:

$$v = \left(\frac{E}{\rho_d} \right)^{1/2}. \quad (2)$$

Figure 4 shows nanoindentation measurements (Nanoindenter DCM, Agilent-MTS) on two a-IGZO films with thicknesses of 200 and 1000 nm. The measured Young's modulus decreased with increasing indentation depth in both measurements. That is affected by the soft glass substrate under the hard film. The Young's modulus of the a-IGZO films is determined as about 130 GPa using very narrow plateau around indentation depth of 20 and 40 nm for the 200 and 1000-nm-thick films, respectively. Using this Young's modulus, Eqs. (1) and (2), l_{ph} was calculated as shown in Table II. The l_{ph} value of the a-IGZO film is 0.35 nm, which is comparable to the nearest neighbor distance of In–In, 0.33 nm.[2] In addition, the l_{ph} value is slightly smaller than the reported l_{ph} value of the a-IZO films, 0.40 nm.[10] Consequently, the l_{ph} value of the a-IGZO film is strongly dominated by a very short range order such as interatomic distance. The λ_{ph} value of the a-IGZO film is smaller than that of the a-IZO film, which is attributed to the l_{ph} magnitude of both TCOs.

In summary, the thermal diffusivity and conductivity of 200-nm-thick a-IGZO films are 5.4×10^{-7} $m^2 \cdot s^{-1}$ and 1.4 $W \cdot m^{-1} \cdot K^{-1}$, respectively, which are constant against a wide carrier density range from 10^{14} to $>10^{19}$ cm^{-3}. Heat in the a-IGZO films is conducted mainly by phonons, and heat conduction carried by electrons is negligible. The thermal conductivity carried by phonons in the a-IGZO films is the smallest among amorphous In_2O_3-based TCOs such as a-ITO and a-IZO films.

Table II. Young's modulus (E), sound velocity (v) and phonon mean free path (l_{ph}) values of a-IGZO and a-IZO films.

Material	λ_{ph} ($W \cdot m^{-1} \cdot K^{-1}$)	E (GPa)	v ($m \cdot s^{-1}$)	l_{ph} (nm)
a-IGZO	1.4	130	4700	0.35
a-IZO[10]	1.85	141	4430	0.40

Acknowledgments The authors thank Dr. Ryo Endoh of Toray Research Centers, Inc. for his X-ray reflection measurement to determine the density of our a-IGZO films.

1) K. Nomura, H. Ohta, A. Takagi, T. Kamiya, M. Hirano, and H. Hosono: Nature **432** (2004) 488.
2) K. Nomura, T. Kamiya, H. Ohta, T. Uruga, M. Hirano, and H. Hosono: Phys. Rev. B **75** (2007) 035212.
3) T. Aoi, N. Oka, Y. Sato, R. Hayashi, H. Kumomi, and Y. Shigesato: Thin Solid Films **518** (2010) 3004.
4) A. Suresh, P. Gollakota, P. Wellenius, A. Dhawan, and J. F. Muth: Thin Solid Films **516** (2008) 1326.
5) W. Lim, J. H. Jang, S.-H. Kim, D. P. Norton, V. Craciun, S. J. Pearton, F. Ren, and H. Shen: Appl. Phys. Lett. **93** (2008) 082102.
6) A. Takagi, K. Nomura, H. Ohta, H. Yanagi, T. Kamiya, M. Hirano, and H. Hosono: Thin Solid Films **486** (2005) 38.
7) M. J. Gadre and T. L. Alford: Appl. Phys. Lett. **99** (2011) 051901.
8) J.-S. Park, T.-W. Kim, D. Stryakhilev, J.-S. Lee, S.-G. An, Y.-S. Pyo, D.-B. Lee, Y. G. Mo, D.-U. Jin, and H. K. Chung: Appl. Phys. Lett. **95** (2009) 013503.
9) M. Ito, C. Miyazaki, M. Ishizaki, M. Kon, N. Ikeda, T. Okubo, R. Matsubara, K. Hatta, Y. Ugajin, and N. Sekine: J. Non-Cryst. Solids **354** (2008) 2777.
10) T. Ashida, A. Miyamura, Y. Sato, T. Yagi, N. Taketoshi, T. Baba, and Y. Shigesato: J. Vac. Sci. Technol. A **25** (2007) 1178.
11) T. Baba: Jpn. J. Appl. Phys. **48** (2009) 05EB04.
12) N. Taketoshi, T. Baba, and A. Ono: Rev. Sci. Instrum. **76** (2005) 094903.
13) T. Yagi, K. Tamano, Y. Sato, N. Taketoshi, T. Baba, and Y. Shigesato: J. Vac. Sci. Technol. A **23** (2005) 1180.
14) T. Yagi, N. Oka, T. Okabe, N. Taketoshi, T. Baba, and Y. Shigesato: Jpn. J. Appl. Phys. **50** (2011) 11RB01.
15) N. Oka, R. Arisawa, A. Miyamura, Y. Sato, T. Yagi, N. Taketoshi, T. Baba, and Y. Shigesato: Thin Solid Films **518** (2010) 3119.
16) R. Endoh, T. Hirano, M. Takeda, M. Oishi, T. Yoshikawa, N. Oka, and Y. Shigesato: Proc. 32nd Japan Symp. Thermophysical Properties, 2011, p. 105.
17) G. V. Samsonov: *The Oxide Handbook* (IFI/Plenum, New York, 1982) 2nd ed., p. 96.
18) E. H. P. Cordfunke and E. F. Westrum: J. Phys. Chem. Solids **53** (1992) 361.
19) T. Ashida, A. Miyamura, N. Oka, Y. Sato, T. Yagi, N. Taketoshi, T. Baba, and Y. Shigesato: J. Appl. Phys. **105** (2009) 073709.
20) S. C. Andrews, M. A. Fardy, M. C. Moore, S. Aloni, M. Zhang, V. Radmilovic, and P. Yang: Chem. Sci. **2** (2011) 706.
21) H. Kaga, R. Asahi, and T. Tani: Jpn. J. Appl. Phys. **43** (2004) 7133.
22) T. Eguchi, H. Inoue, A. Masuno, K. Kita, and F. Utsuno: Inorg. Chem. **49** (2010) 8298.